High Frequency Performance of Graphene Nanoribbon TFETs with Phonon Scattering

Kai-Tak Lam[†], Vijayashree Parsi Sreenivas, Gengchiau Liang[*]
Computational Nanoelectronics and Nano-devices Lab, Department of Electrical and Computer Engineering,
National University of Singapore, 4 Engineering Drive 3, Singapore 117583, Republic of Singapore
e-mail: {[†]lamkt, [*]elelg}@nus.edu.sg

INTRODUCTION

Research in the use of graphene nanoribbon (GNR) in electronic devices has been widely explored since 2004 and many studies of the GNR tunneling FETs (TFETs) have also evaluated their device performance both in the ballistic limits [1], [2] and in the context of phonon scattering [3], [4] for digital applications. In this work, we present our study of the high frequency device performance of GNR TFETs using a non-equilibrium Green's function (NEGF) quantum simulator with a mode-space Dirac equation model. We simulated GNR TFETs of different ribbon widths in the ballistic limits, as well as in the presence of phonon scattering. It was observed that with the inclusion of phonon scattering, the current of the TFETs generally increases due to the enhanced band-to-band (BTB) tunneling and the ON-/OFF-state current ratio (I_{ON}/I_{OFF}) and the subthreshold swing were degraded. As a result, the transconductance (g_m) was reduced, which led to a lower operation frequency (f). Conversely, the drain conductance was increased due to the phonon assisted BTB tunneling at the channel-drain interface, resulting in a lower gain (A_v). Lastly, A_v decreased and f increased with an increasing ribbon width (W) of the GNR TFETs.

METHODOLOGY

A schematic of the device simulated in this study and the band diagram of GNR TFETs at OFF-state is shown in Fig. 1(a) and 1(b), respectively. GNRs with W = 1.0, 1.8 and 4.0 nm, and energy bandgaps (E_G) of 0.87, 0.55 and 0.25 eV, respectively, are studied. The retarded Green's function G^r in the NEGF formulism is obtained via [5]

$$G^r = \left[EI + i\eta - H_0 - U - \Sigma_S - \Sigma_D - \Sigma_{ph} \right]^{-1} \tag{1}$$

The device Hamiltonian H_0 is described with the mode-space Dirac equation [1] and the Σ_S and Σ_D are the self-energies of the source and drain. The phonon scattering component represented by Σ_{ph}, is obtained by the sum of in- and out-scattering self-energies based on the self-consistent Born approximation [5], [6]

$$\Sigma_{ph}^{in/out}(E) = \int \Big\{ D^{ab}(\hbar\omega)\left[N(\hbar\omega)+1 \right] G^{n/p}(E \pm \hbar\omega) + D^{em}(\hbar\omega) N(\hbar\omega) G^{n/p}(E \mp \hbar\omega) \Big\} d\omega \tag{2}$$

The electron-phonon coupling constants $D^{ab} = D^{em} = D$ are obtained following Ref. 4 and for W = 1.0 nm, the acoustic phonon (AP), $D_{AP} = 3.1\times10^{-3}$ eV^2 and the optical phonon (OP), assuming only phonons with energy $\hbar\omega$ = 0.19 eV are significant, $D_{OP} = 1.30\times10^{-2}$ eV^2. Different values for the different W are used [4]. For the high frequency performance,

$$g_m = \frac{dI_{DS}}{dV_{GS}},\ g_d = \frac{dI_{DS}}{dV_{DS}},\ A_v = \frac{g_m}{g_d},\ f = \frac{g_m}{2\pi C_G}. \tag{3)-(6}$$

DISCUSSION

We focused firstly on 1.0 nm wide GNR TFET. The current characteristics of the device in ballistic condition and in the presence of phonon scattering are shown in Fig. 2(a) and 2(b) respectively. In the former case, as the drain bias (V_{DS}) increased, the ambipolar behavior of TFETs became significant due to the increasing BTB tunneling at the channel-drain interface at small gate bias (V_{GS}). The drain current (I_{DS}) was higher with phonon scattering due to the phonon-assisted BTB tunneling at the channel-drain interface within low V_{GS} region, and at the source-channel interface within high V_{GS} region. The presence of phonon scattering degraded both the I_{ON}/I_{OFF} and the sub-threshold swing of the GNR TFET.

The g_m was next calculated for both conditions and they are shown in Fig. 2(c) and 2(d). Due to the reduced I_{ON}/I_{OFF}, the change in I_{DS} with respect to V_{GS} decreased with phonon scattering and the g_m was lowered in general. Conversely, the g_d, shown in Fig. 2(e) and 2(f), increased with phonon scattering in general except for the low V_{DS} and high V_{GS} region, where the increase in V_{DS} did not increase the BTB tunneling at the channel-drain interface significantly due to the large E_G of 1.0 nm GNR. The A_v and f were then calculated, with the gate capacitance (C_G) obtained from the change in the channel charge at different V_{GS}, and they are shown in Fig. 3 in log-scale. At V_{DS} = 0.3 V (dash line), the A_v first increased then decreased, while the f increased monotonously, as V_{GS} increased. In general, both A_v and f degraded in the presence of phonon scattering.

Lastly, the I_{DS}, A_v and f of GNR TFETs with various widths are shown in Fig. 4 for both ballistic and phonon scattering conditions at V_{DS} = 0.3 V. For W = 0.4 nm, due to the small E_G, the device was at ON-state for all V_{GS}. Choosing a V_{GS} = 0.3 V, for both ballistic and phonon scattering conditions, A_v decreased and f increased as W increased, as shown in the insets of Fig. 4(b) and 4(c).

CONCLUSION

A computation study on the high frequency performance of different widths GNR TFETs with phonon scattering is presented here and both A_v and f were degraded in the presence of phonon. As W increased, A_v decreased and f increased for both conditions.

ACKNOWLEDGEMENT

This work was supported by A*STAR PSF Grant 082101002.

REFERENCES

[1] S.-K. Chin, et al., IEEE Trans. Elec. Dev. **57**, 3144 (2010).
[2] K.-T. Lam, et al., IEEE Elec. Dev. Lett. **32**, 431 (2011).
[3] Y. Ouyang, et al., Appl. Phys. Lett. **92**, 243124 (2008).
[4] S. O. Koswatta, et al., IEEE Trans. Elec. Dev. **56**, 456 (2009)
[5] S. Datta, Quantum Transport (2005) Chapter 10
[6] D. Nikonov, et al., (2009) http://nanohub.org/resources/7772

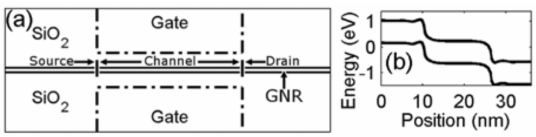

Fig. 1. (a) Schematics of GNR TFETs with a double metal gate structure and silicon dioxide (SiO_2) as the dielectric. The gate oxide thickness is 1.0 nm and the channel length is 16 nm. (b) The band diagram of a 1.0 nm wide GNR TFET with *p*-type source and *n*-type drain. The doping concentration is at 4.47×10^{13} cm^{-2}.

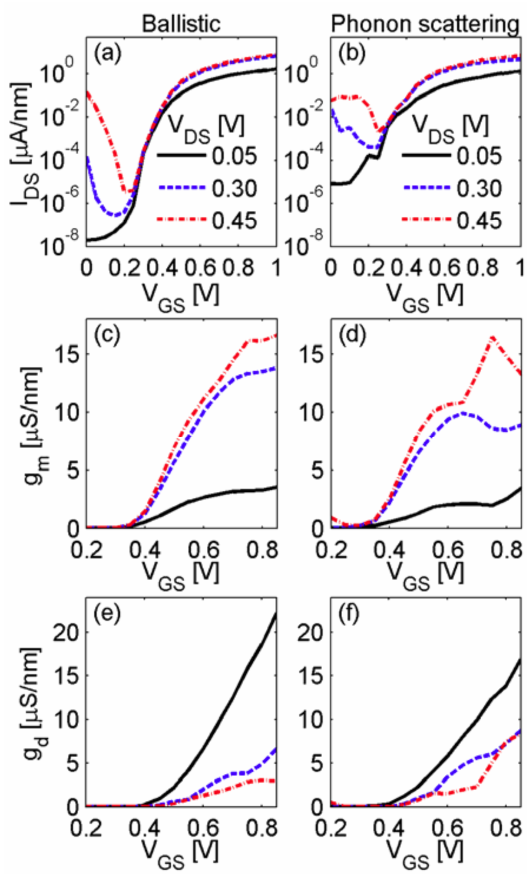

Fig. 2. The current characteristics of GNR TFET (W = 1.0 nm) at (a) ballistic condition and (b) with phonon scattering. The transconductance (g_m) and drain conductance (g_d) are shown in (c)-(f) for both conditions. The bias step for the conductance calculations was set at 2 mV. The drain bias (V_{DS}) ranged from 0.05 to 0.45 V were calculated and only V_{DS} = 0.05, 0.30 and 0.45 V are shown here.

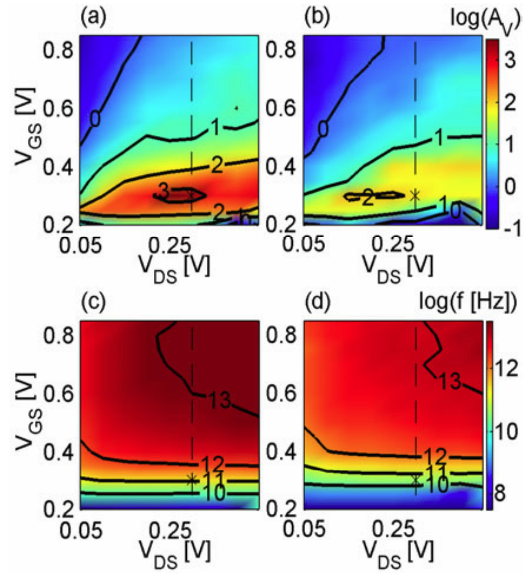

Fig. 3. The contour plots of gain (A_v) in log-scale for (a) ballistic and (b) phonon scattering conditions. The colorbar besides (b) applies to both figures. The (blue) regions less than 0 indicate A_v < 1 and the device should not be operated as an amplifier under these biasing conditions. The contour plots of operation frequency (f) in log-scale for (c) ballistic and (d) phonon scattering conditions. The dash lines in all figures represent V_{DS} = 0.3 V and the crosses indicate V_{GS} = 0.3 V.

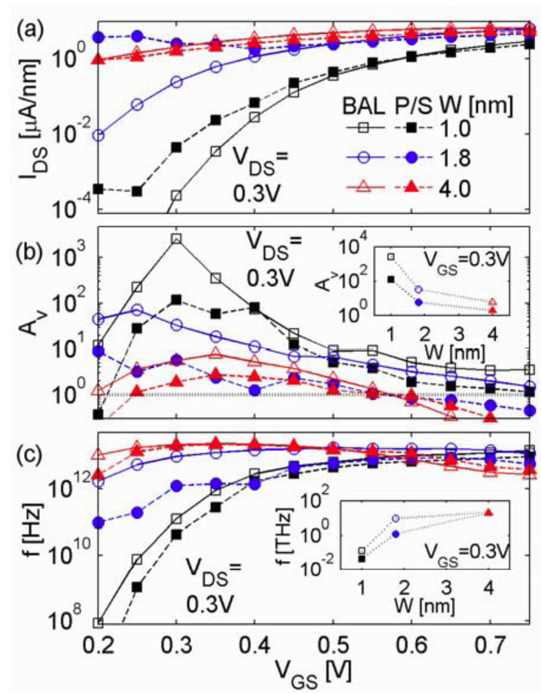

Fig. 4. (a) The transfer characteristics, (b) A_v and (c) f of different width (W) GNR TFETs as a function of V_{GS} at V_{DS} = 0.3 V for ballistics (BAL) and phonon scattering (P/S) conditions. The currents in phonon scattering conditions generally increased except for W = 4.0 nm where the device was in ON-state for all V_{GS} at V_{DS} = 0.3 V. The dotted line in (b) indicates A_v = 1. Insets in (c) and (d) show the variation in of A_v and f with respect to W.